Femtosecond Transient Absorption Study of the Dynamics of Acrylodan in Solution and Attached to Human Serum Albumin

Andrea Buzády,*,†,‡ Janne Savolainen,§ János Erostyák,† Pasi Myllyperkiö,§ Béla Somogyi,‡ and Jouko Korppi-Tommola*,§

Department of Experimental Physics, Institute of Physics, University of Pécs, Ifjúság u. 6., H-7624 Pécs, Hungary, Department of Biophysics, University of Pécs, Szigeti út 12., H-7625 Pécs, Hungary, and Department of Chemistry, University of Jyväskylä, P.O. Box 35, FIN-40351 Jyväskylä, Finland

Received: October 1, 2002; In Final Form: November 25, 2002

The excited-state relaxation dynamics of the protein-labeling dye acrylodan in solution and attached to human serum albumin has been studied by femtosecond transient absorption spectroscopy. Time-resolved spectra and kinetics of stimulated emission and excited-state absorption in the wavelength region from 400 to 800 nm were studied in ethanol and dimethylformamide. The excited-state solvation dynamics is characterized by multiexponential behavior in both solvents. In ethanol solution, the time dependence of the transient spectra is interpreted in terms of fast solvent relaxation followed by excited-state isomerization of the dye. Acrylodan attached to the protein shows a relaxation component of 3 ps that is attributed to the solvation dynamics of water in the neighborhood of the fluorescent label.

Introduction

Femtosecond spectroscopy has proven to be an efficient technique with which to study protein dynamics. Both fluorescence upconversion[1−3] and transient absorption[4,5] methods have been widely applied. Intramolecular charge transfer,[4] ultrafast isomerization[2], solvation dynamics,[1] and resonance energy transfer[1] in proteins have been characterized. Time scales involved in protein dynamics may vary by several orders of magnitude from femtoseconds to milliseconds. Femtosecond excitation of a protein chromophore often results in multiexponential behavior of the excited-state dynamics. Reorientation or isomerization of the chromophore, solvent dynamics near the binding site, or nuclear motions of the local protein environment may give rise to multiexponential relaxation. It is often very difficult to assign the observed nonexponential kinetics conclusively to these various processes. Besides stochastic relaxation, coherent oscillations in the early part of the relaxation signal may be observed. Coherent effects can be studied when energy dissipation towards other degrees of freedom occurs on a timescale that is long enough compared to the damping time of the initially prepared oscillations.

Both intrinsic (e.g., tryptophan) and extrinsic fluorophore groups are used for the characterization of the local dynamics of biological macromolecules. Nonexponential relaxation of tryptophan in proteins may cover a wide time range, from subpicoseconds to nanoseconds.[1]

By attaching an extrinsic dye probe to a protein, the solvation dynamics of polar amino acid residues or rigid water molecules have been reported.[6,7] The binding of ligands to hydrophobic sites of human serum albumin (HSA) has been extensively studied.[8−10] Evidence of proton transfer and intramolecular twisting of the label attached to the protein was observed.[2]

In a protein environment, the multiexponential behavior of dynamics has been observed, and these results have been explained using different assumptions. The experimental results are generally described by supposing the reorientation of bulk solvent, reorientation of the protein environment, relaxation of bound solvent molecules, and the inertial motion and diffusion of solvent and/or solute molecules.

HSA has been of interest for decades. It has many physiological functions involving transport and bindings. It delivers fatty acids, steroids, and other molecules. Drugs and drug metabolites can interact covalently with HSA, and thiol-containing drugs can bind to the single free cysteine residue (Cys-34) of HSA.[9] The reversible binding of ligands can be stereospecific, and thus immobilized HSA can be used to separate drug isomers. It is possible to probe the local HSA dynamics around this Cys-34 residue using a site-specific labeling method.

We have used the sensitive solvatochromic probe 6-acryloyl-2-dimethylaminonaphthalene (Acrylodan, AC) that was developed for labeling free cysteine residue in proteins.[13] AC has a broad fluorescence emission spectrum with a maximum position depending strongly on the polarity of its environment (between 470 and 560 nm). Reorientational motion and intra- and intermolecular energy transfer of a number of proteins labeled with AC have been studied at subnanosecond and nanosecond time resolutions.[11−22] Many of these investigations focused on the details of the denaturation steps of the labeled proteins. Their time resolution allowed for the discovery of the details of the protein motions (using Stokes shift measurements) and the rotational components of the probe and the protein (using anisotropy measurements).

The excitation of a label attached to a protein may result in a relaxation signal that contains a wide distribution of time constants from picoseconds to tens of nanoseconds.[23−27] Our

* Corresponding authors. E-mail: buzady@fizika.ttk.pte.hu, ktommola@jyu.fi.
† Department of Experimental Physics, University of Pécs.
‡ Department of Biophysics, University of Pécs.
§ University of Jyväskylä.

10.1021/jp027107o CCC: $25.00 © 2003 American Chemical Society
Published on Web 01/11/2003

recent studies[22] have shown time components from subnanosecond to nanosecond timescales with at least one component shorter than 10 ps for AC attached to HSA (HSA/AC). To obtain further information on the fast processes, femtosecond transient spectroscopy was employed. To obtain background information for the interpretation of the dynamics of AC attached to the Cys-34 amino acid residue of HSA, the electronic relaxation of AC in simple solvents was studied first. The dye in solution and attached to the protein shows excited-state absorption (ESA) and stimulated emission (SE) in the spectral region, where there is no ground-state absorption. Hence, direct evidence of the initially prepared excited-state depopulation was obtained by recording transient signals in these spectral regions. Solvation dynamics of AC in solution and the dye in ethanol and in dimethylformamide were studied first. In these solvents, the spectral position of AC's emission is similar to that of HSA/AC, which is indicative of the similar polarity of the AC's environment both in the solutions mentioned and attached to HSA. With these results in hand, information on local protein motions and solvation dynamics around the hydrophobic binding site of the label (near Cys-34 of HSA) could be obtained. The observed spectroscopic effects refer to the immediate surroundings of the probe (i.e., the hydration water molecules and the protein groups in the vicinity. The global protein motions cannot be detected on the time scales used in our experiments.

Experimental Section

Acrylodan was purchased from Molecular Probes. Spectroscopic grade dimethylformamide (DMF) and ethanol were used as solvents. The concentrations of solutions were adjusted to absorbancies from 0.3 to 0.6 in a 1-mm cell. Steady-state absorption and fluorescence measurements were carried out with a Shimadzu UV 2100 spectrophotometer and a Jobin-Yvon Florolog τ3 spectrofluorometer, respectively, at the University of Pécs.

HSA was purchased from Sigma (code: A 3782) and used without further purification. Prior to this work, this essentially fatty acid-free (<0.005%), globulin-free material was tested after further purification, but no change of spectroscopic parameters was found. The labeling of HSA was done using Wang's method[15] with a minor modification.[22] Briefly, the protein solution containing 7.24×10^{-5} M HSA was prepared in 0.1 M sodium phosphate buffer of pH 7.0. AC (the molar ratio was 1:1) was freshly dissolved in 50 μL of DMF and added to the HSA/buffer solution under gentle stirring. The mixture was allowed to react for 6 h at room temperature. It was then loaded into a dialysis bag and dialyzed at 4 °C against 0.1 M sodium phosphate buffer of pH 7.0. After 4 days of changing the buffer every 12 h to remove any residual free AC, the HSA/AC solution was passed through a Sephadex G-25 column.

Transient signal measurements were carried out in the laser laboratory of the University of Jyväskylä. Femtosecond seed pulses were generated in a Ti/sapphire oscillator (Coherent Mira 900) pumped by a diode-pumped frequency-doubled YAG laser (Coherent Inc., Verdi-5W). Seed pulses were amplified in a 1-kHz regenerative amplifier system (pump laser Quantronix Inc. 527 frequency-doubled 1-kHz YLF laser, model 4800 regenerative amplifier, model 4820 stretcher and compressor both from Quantronics Inc.). Fundamental femtosecond pulses with a central wavelength of 795 nm, 180-fs pulse duration, and 550-μJ pulse energy were generated in the amplifier. Part of the fundamental beam was frequency doubled (397 nm) and used as a pump. The typical pump energy at the sample was 1.5 μJ/pulse. Part of the fundamental beam was focused onto a 2-mm sapphire window to generate a white-light continuum. About a 5-nm bandwidth from the continuum was used to probe the excitation and transmission in the spectral range from 460 to 760 nm. The beam of white light was split into two beams: 50% was used to probe the excitation (overlap with the pump), and the other 50% was used to measure the transmission of the sample. The polarization of the pump beam was set at the magic angle (54.7°) with respect to the probe beam. For data acquisition, the peak intensity of each laser pulse was digitized and recorded using a detector system consisting of a monochromator ($\Delta\lambda = 6$ nm) and three photodiodes interfaced to a personal computer via preamplifiers, sample and hold circuitry, A/D conversion, and a multiplexer. The recorded transient signal did not exceed 6 ΔmOD.

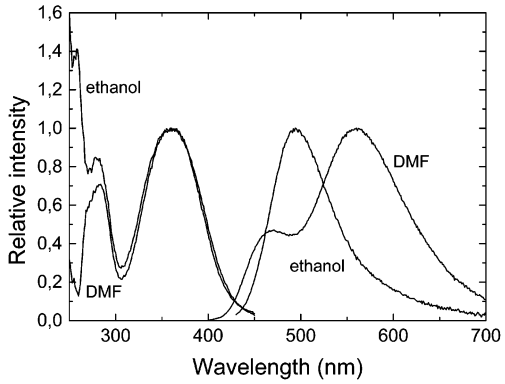

Figure 1. Steady-state excitation and emission spectra of AC.

The pulse width was obtained by measuring the optical Kerr signal in pure ethanol and by deconvolving the signal assuming a Lorentzian pulse shape.

Transient signal matrices were constructed by using the information contained in a number of recorded decay curves measured at 20-nm wavelength intervals. In the pump and probe recordings, a variable stepping of the delay line was used. Transient spectra were obtained by plotting ΔOD as a function of wavelength at fixed time delays. Time zeros at each wavelength were determined by using white light and the optical Kerr signal in ethanol. A polynomial fitting was used to obtain time-zero corrections at each wavelength.

Results and Discussion

Figure 1 shows the steady-state excitation and emission spectra of AC in solution. The spectrum of the excitation pulse centered at 397 nm overlaps the red side of the lowest-energy absorption band of the dye and populates the first excited singlet state (S_1). At wavelengths longer than 450 nm, there is practically no ground-state absorption.

AC in DMF Solution. The steady-state emission spectrum of AC in DMF exhibits two maxima: one at 460 nm and other at 560 nm. In the spectral region from 450 to 750 nm, the negative ΔOD transient signal originates from stimulated emission, and the positive transient signal is due to excited-state absorption.

Figure 2 shows a 2D presentation of the transient signal matrix of AC in DMF over the wavelength region from 460 to 760 nm in the time frame from zero to 38 ps. Figure 3a−c shows the time behavior of the recorded transient spectra up to 350 ps. Immediately after excitation, two wide bands—a strong, negative SE band peaking at 520 nm and a positive ESA band with a maximum at 675 nm—appear in the transient spectrum.

Both of these bands decay rapidly during the first few picoseconds and reach a slower decay phase after about 5 ps.

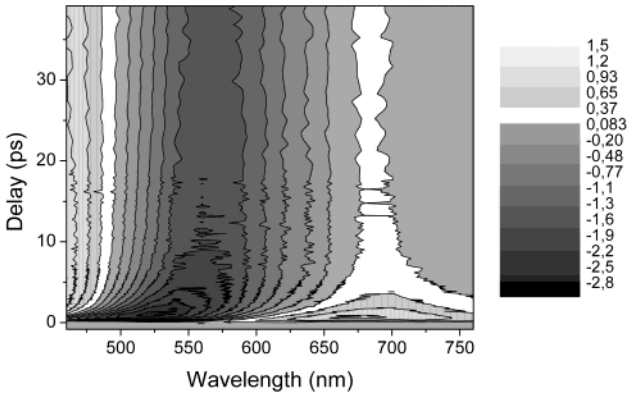

Figure 2. Contour plot of the transient signal matrix of AC in DMF.

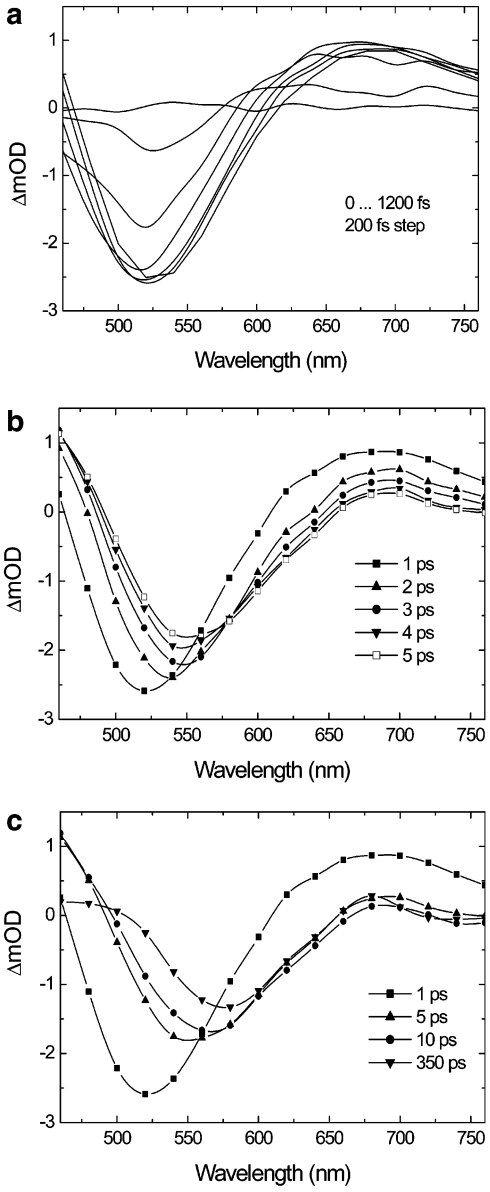

Figure 3. (a−c) Evolution of the transient spectra of AC in DMF.

The fast decay takes about 1.4 ps. As shown in Figures 2 and 3, the stimulated emission spectrum shifts rapidly toward longer wavelengths. This fast Stokes shift is attributed to the solvation relaxation of the excited S_1 state. Parallel to these changes, an ESA band also appears at shorter wavelengths (<480 nm). The formation of this band takes about 5 ps.

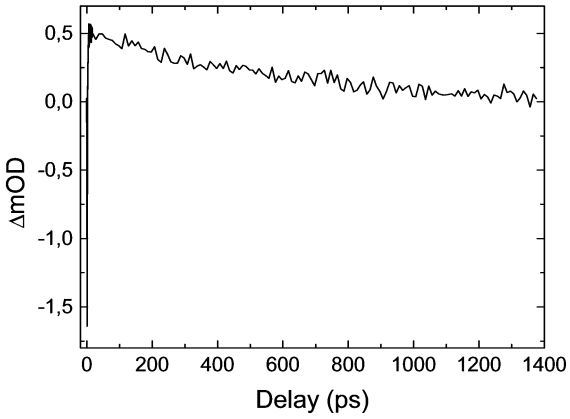

Figure 4. Transient signal of AC in DMF on a longer timescale measured at $\lambda = 480$ nm.

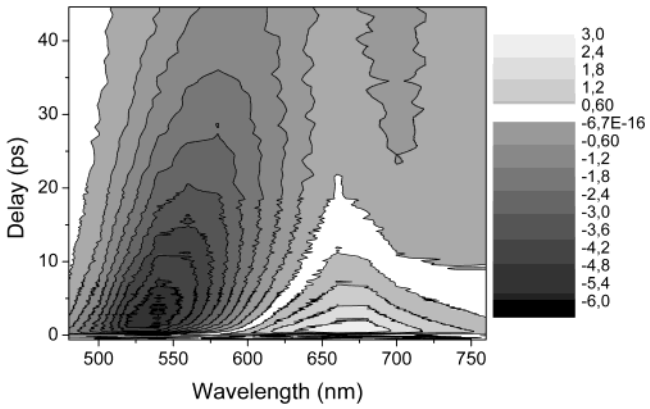

Figure 5. Contour plot of the transient signal matrix of AC in ethanol.

To see the long timescale behavior of the transient spectra, the decay at $\lambda = 480$ nm was measured over a delay of about 1.4 ns (Figure 4). After excitation, a rapidly rising negative signal quickly turns into a positive excited-state absorption signal that finally decays in about 620 ps.

AC in Ethanol Solution. The steady-state emission spectrum of AC in ethanol shows a broad band centered at about 495 nm.

The same kind of structureless emission spectrum is also observed when AC is attached to water-soluble proteins. Figure 5 shows a 2D presentation of the transient signal matrix recorded for AC in ethanol solution. Figure 6a−d shows the time dependence of the transient spectra up to 350 ps.

Transient spectra of AC in DMF and in ethanol solutions show some similarities and some differences. Immediately after excitation in ethanol, a strong SE band with a maximum at 530 nm and an intensive ESA band at 670 nm appear. Both of these bands decay in 4.2 ps. In the time frame from 1 to 5 ps, the shift of the SE band toward longer wavelengths is less dramatic in ethanol solution than in DMF. The initial fast Stokes shift in ethanol is attributed to the excited-state solvent relaxation of the dye. In ethanol solution, the blue ESA band appears at wavelengths shorter than 500 nm.

The transient spectra in ethanol shift further to 560 nm about 20 and 350 ps after the excitation, and almost zero delta absorption is observed (Figure 6d). The SE signal is overlapped with a wide, new ESA band appearing at a later time in the spectrum between 520 and 760 nm. By this time, the short-wavelength ESA has disappeared, and SE can be seen only in a narrow spectral region from 470 to 510 nm.

A decay signal measured at $\lambda = 600$ nm over a long time delay supports this interpretation (Figure 7). After excitation, a

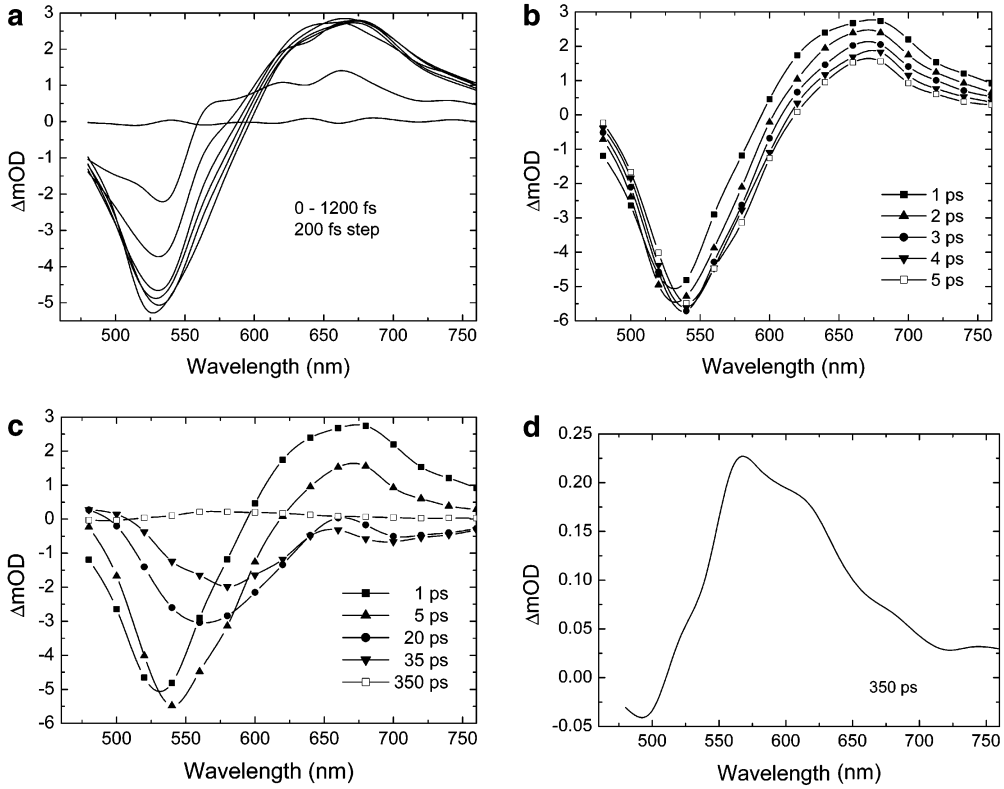

Figure 6. (a−d) Evolution of the transient spectra of AC in ethanol.

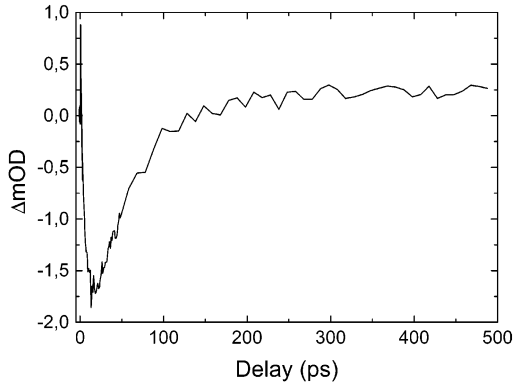

Figure 7. Transient signal of AC in ethanol on a longer timescale measured at $\lambda = 600$ nm.

fast-rising positive signal is seen, followed by a rapid change to a negative signal. The first positive signal arises from early-time ESA, which decays rapidly. At the same time, the SE band moves toward longer wavelengths. These two effects result in the appearance of a strong negative signal. The negative transient signal becomes positive in about 50 ps and reaches a maximum ESA after 350 ps, which then decays in nanoseconds.

Solvation Dynamics. From the measured transient spectra of AC in ethanol and in DMF, it is obvious that there are many competing processes taking place in solution on timescales from femtoseconds to nanoseconds. Excited-state solvation relaxation is the most probable origin of the observed fast initial spectral shifts. Solvent relaxation kinetics may be obtained by evaluating the time dependence of the shift of the SE band. A dynamic Stokes shift is usually characterized by the normalized spectral response function[29]

$$C(t) = \frac{\nu(t) - \nu(\infty)}{\nu(0) - \nu(\infty)} \qquad (1)$$

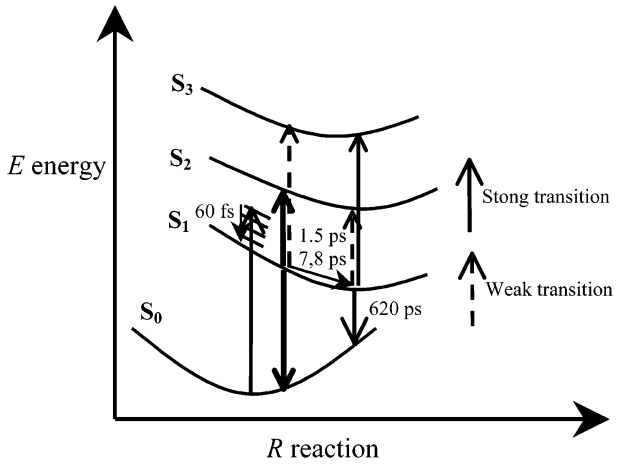

Figure 8. Proposed energy scheme for AC−DMF solution.

where $C(t)$, in linear response theory, represents the solvation correlation function of solvent-induced fluctuations of the optical transition frequency. In eq 1, $\nu(t)$ is the first moment of the spectral band experiencing the solvent shift. Equation 1 may be rewritten as

$$\nu(t) = \nu(0) + [C(t) - 1]\Delta\nu \qquad (2)$$

where $\Delta\nu = \nu(0) - \nu(\infty)$. The fitting of $\nu(t)$, the parameters $\nu(0)$ and $\Delta\nu$, and the time-evolution function $C(t)$ can be calculated. In the simplest case, $C(t)$ is monoexponential, but in many cases, it shows distributed characteristic time behavior.

The kinetic results for AC in DMF solution are interpreted according to the schematic potential energy diagram shown in Figure 8. Vibrational relaxation is assumed to be over in about 60 fs, within the time resolution of our experiment (fwhm = 180 fs). Figure 9 displays the time dependence of the spectral shift of the SE band with time zero at $\nu(0) = 21\,300$ cm^{-1} (470

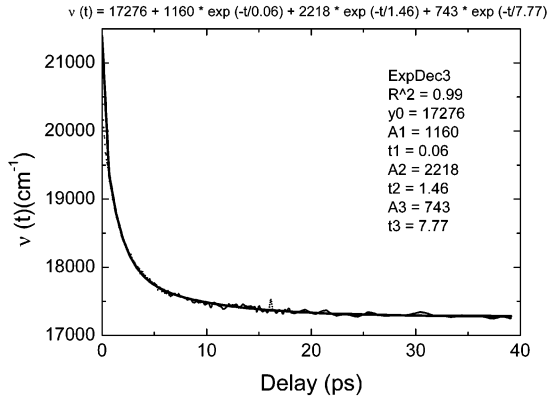

Figure 9. Time dependence of the first moment of the SE band measured in the AC−DMF system.

nm). The $C(t)$ function was fitted with three exponentials. The fastest resolved component (60 fs) is attributed to vibrational cooling.

Two picosecond components (1.5 and 7.8 ps) are assigned to excited-state solvation equilibration. In about 15−20 ps, the solvation relaxation is over. It is interesting that under the time of solvation not only the center of gravity of the SE band moves toward red but also the amplitude of the signals decreases. This means that SE has the highest transition probability right after excitation. Later, this probability decreases quickly as the solvent molecules−solute molecule system moves toward its new equilibrium position.

The long-wavelength ESA ($S_1 \rightarrow S_2$) band decays in 1.4 ps, at a similar rate as that of the early part of the SE decay. The red ESA is attributed to the $S_1 \rightarrow S_2$ transition (Figure 8). It reaches a slowly decaying state as the molecules come to equilibrium in the S_1 state. A short-wavelength ESA band evolves simultaneously with the SE and the red ESA bands. This band is attributed to the $S_1 \rightarrow S_3$ transition. In Figure 2, only the long-wavelength end of this blue ESA band can be seen ($\lambda < 480$ nm). Two possible explanations can be given: (a) as solvation proceeds, the transition probability between the S_1 and S_3 levels increases or (b) the $S_1 \rightarrow S_3$ transition has a constant cross section at all times, but the cross section of SE ($S_1 \rightarrow S_0$) is much higher during the first few picoseconds.

After the completion of solvation, the molecules remain in equilibrium in the S_1 state. The transient-signal spectrum measured 350 ps after the excitation is almost identical to the spectrum measured about 30 ps after excitation (Figure 3c). In summary, the wavelength region that was studied involved three timescales of events that were observed. After the vibrational cooling in femtoseconds, solvation relaxation occurs during the first few picoseconds after excitation and is followed by $S_1 \rightarrow S_0$ emission with a lifetime of 620 ps.

A simplified potential energy scheme for AC in ethanol is shown in Figure 10. In ethanol, the 200-fs time component of the $\nu(t)$ curve is assigned to vibrational cooling (Figure 11) (time zero wavenumber $\nu(0) = 20\,800$ cm^{-1}, 480 nm). The second component of 3.8 ps is due to solvent reorientational relaxation after excitation.

The decays of the SE band at 530 nm and the red ESA band at 660 nm and the rise of the blue ESA band at 480 nm all occur in 8 ps. The same kinetic constant implies that the time dependencies of SE, red ESA, and blue ESA bands are connected to the same level, namely, S_1. It seems that the oscillator strengths of the $S_1 \rightarrow S_0$ transition (SE band) and the $S_1 \rightarrow S_2$ transition (red ESA band) decrease whereas that for

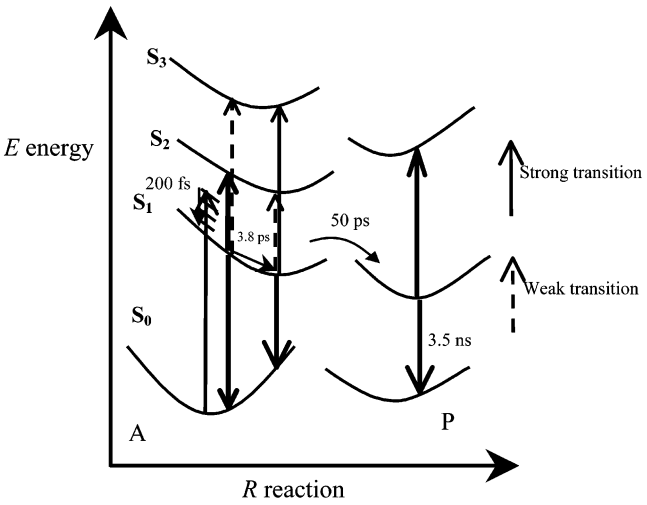

Figure 10. Proposed energy scheme for the AC−ethanol system.

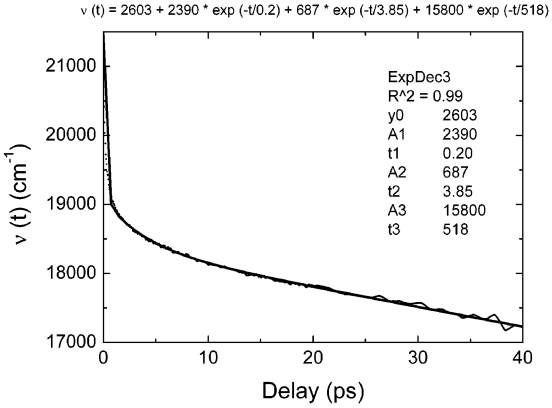

Figure 11. Time evolution of the first moment of the SE band measured in the AC−ethanol system..

the $S_1 \rightarrow S_3$ transition increases (blue ESA band) as solvation proceeds.

After the first 15 ps, the transient signal of AC in ethanol solution continues to change. This can be seen in Figures 5 and 6. The transient signal within the SE band in ethanol solution does not approach zero, but becomes positive, which means that a new ESA band is building up in about 50 ps. It is likely that there is an overlap of spectral features of opposite sign (the SE and the emerging ESA band) in the region from 520 to 550 nm.

We attribute these changes to the formation of a new photoproduct (PP), a new isomer of AC in the excited S_1 state. The isomer probably gives rise to a broad excited-state absorption observed at 560 nm.

The fit of the $\nu(t)$ (Figure 11) curve gives 518 ps as a third time constant for the shift kinetics. This is a result of a continuing shift of the SE band, the disappearance of the red ESA band, and the appearance of the blue ESA band. This 518-ps time constant is an apparent one; it must not be attributed to one process (e.g., solvation alone).

Dielectric Relaxation of AC Attached to HSA. Because HSA/AC is a photosensitive complex, the pump intensity was reduced, and the transient signal was kept below 0.7 ΔmOD. The spectral and time evolution of the SE band between 450 and 540 nm was recorded. Figure 12 shows three representative decays of the SE band.

It can be clearly seen that the signal decays on the blue side and rises on the red side of the SE band. Figure 13 displays the time dependence of the spectral shift of the SE band.

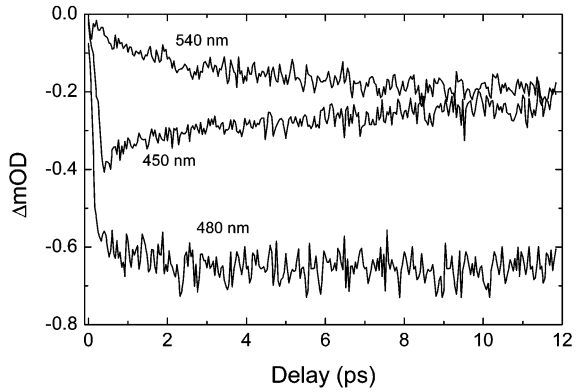

Figure 12. Three representative decays at the blue side, the top, and the red side of the SE band in HSA/AC.

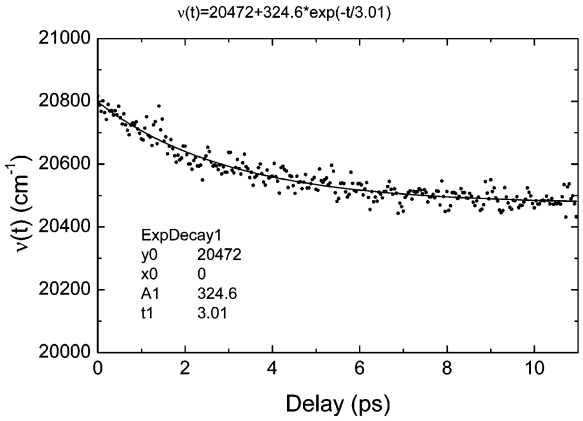

Figure 13. Time evolution of the first moment of the SE band in HSA/AC.

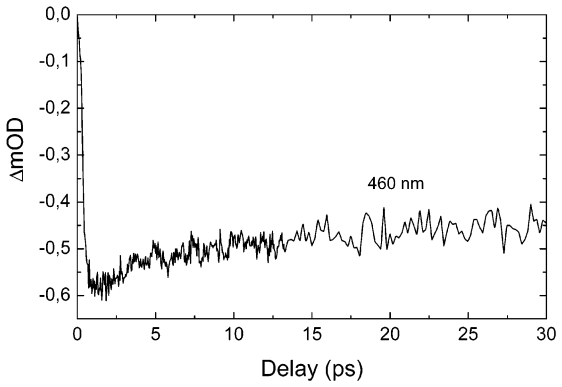

Figure 14. Transient signal measured at $\lambda = 460$ nm in HSA/AC.

A single-exponential fit gives a characteristic time constant of relaxation of 3.0 ps (Figure 13). This time constant was observed but not calculated exactly in former fluorescence emission measurements.[22]

Figure 14 shows the transient signal of AC bound to HSA recorded at 460 nm, in the region of SE of the label.

Fast relaxation takes place in 10−15 ps, and then the SE signal reaches a constant level reflecting the long-time behavior, which is assigned to the emission lifetime of AC bound to the protein, which was previously determined by phase-fluorometry measurements.[22] In contrast to positive subnanosecond-scale transient signals recorded for AC in solution in the wavelength region around 480 nm (Figure 4), a negative signal was obtained for AC attached to HSA. This means that when the dye interacts with the protein, the excited-state absorption of S_1 to S_3 is reduced.

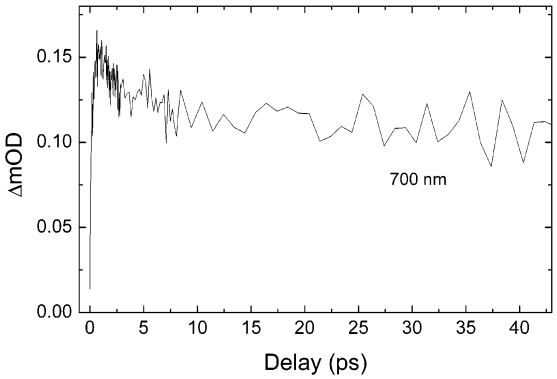

Figure 15. Transient signal measured at $\lambda = 700$ nm in HSA/AC.

For AC in solution, a positive ESA signal was found between 650 and 720 nm, which is also present in HSA/AC as shown in Figure 15.

Conclusions

The time evolution of the transient signal spectra of acrylodan in DMF and ethanol was measured. Several ultrafast processes take place in the excited AC molecules in solution. The beginning part of vibrational cooling was not resolved but was recognized as an initial detuning of the transient spectra from the wavelength of the excitation light. The resolved, initial femtosecond excited-state relaxation in solution (60 fs in DMF and 200 fs in ethanol) is assigned to vibrational relaxation. In DMF solution, two time constants (1.5 and 7.8 ps) are assigned to solvation relaxation around excited AC. This deviation from exponentiality of the solvation relaxation was observed by many authors.[12,28,30] The slower phases of solvation vary strongly from solvent to solvent. In ethanol solution, a solvation relaxation component of 3.8 ps was determined. A much longer scale shift of $\nu(t)$, resulting in an apparent component, was resolved. An additional effect characterized by 50 ps, which was not present in DMF, was observed in ethanol solution. It was assigned to the isomerization of AC in the excited state.

In accordance with other studies,[28,31] a slower and more evenly distributed relaxation was found in ethanol solution. In the case of the AC-like compound laurdan in ethanol,[31] the initial excited states were supposed to evolve through unrelaxed and relaxed charge transfer states on the picosecond timescale.

A relaxation component of 3.0 ps for AC attached to HSA was determined. This relaxation is attributed to the solvation of water molecules in the hydrophobic binding pocket of the protein. Other studies have shown that confined water molecules have slower solvation times than bulk water because of the hindered motion of the molecules.[32,33] This fact explains why this fastest relaxation component of 3.0 ps is otherwise at least 1 order of magnitude slower than in the case of probes in bulk water. The next relaxation components observed in HSA/AC,[22] which are much slower (400 ps−10 ns), belong to both the slow dielectric relaxation of the protein environment around the probe molecule attached to HSA via the Cys-34 amino acid residue and to the global protein motions.

Besides the characterization of the time evolution of the dielectric relaxation, a fast change in the transition probabilities was observed. Both in DMF and ethanol solutions, the probabilities of the $S_1 \rightarrow S_2$ and $S_1 \rightarrow S_0$ transitions decrease and the probability of the $S_1 \rightarrow S_3$ transition increases. The characteristic times for these changes are 1.4 ps in DMF and 4.2 ps in ethanol.

It was also found that when the dye interacts with the protein the probability of $S_1 \rightarrow S_3$ excited-state absorption is reduced.

This means that SE has the highest transition probability right after excitation. Later, this probability decreases quickly as the solvent molecules−solute molecule system moves toward its new equilibrium position.

Acknowledgment. Financial support from the ESF-ULTRA femtochemistry and biology program is gratefully acknowledged (A.B. and J.E.) This work was also supported by the Hungarian National Scientific Research Foundation (grant nos. T032700 and T034443) and by the Finnish Academy of Sciences (contract no. 50670).

References and Notes

(1) Zhong, D.; Pal, S. K.; Zhang, D.; Chan, S. I.; Zewail, A. H. *Proc. Natl. Acad. Sci. U.S.A.* **2002**, *99*, 13.

(2) Zhong, D.; Douhal, A.; Zewail, A. H. *Proc. Natl. Acad. Sci. U.S.A.* **2000**, *97*, 14056.

(3) Kandori, H.; Furutani, Y.; Nishimuar, S.; Shichida, Y.; Chosrowjan, H.; Shibata, Y.; Mataga, N. *Chem. Phys. Lett.* **2001**, *334*, 271.

(4) Wan, Ch.; Fiebig, T.; Schiemann, O.; Barton, J. K.; Zewail, A. H. *Proc. Natl. Acad. Sci. U.S.A.* **2000**, *97*, 14052.

(5) Hamanaka, Y.; Kurasawa, H.; Nakamura, A.; Uchiyama, Y.; Marumoto, K.; Kuroda, S. *J. Lumin.* **2001**, *94*−*95*, 451.

(6) Jordanides, X. J.; Lang, M. J.; Song, X.; Fleming, G. R. *J. Phys. Chem B* **1999**, *103*, 7995.

(7) Changenet-Barret, P.; Choma, C. T.; Gooding, E. F.; DeGrado, W. F.; Hochstrasser, R. M. *J. Phys. Chem B* **2000**, *104*, 9322.

(8) Krishnakumar, S. S.; Panda, D. *Biochemistry* **2002**, *41*, 7443.

(9) Kragh-Hansen, U.; Chuang, V. T.; Otagiri, M. *Biol. Pharm. Bull.* **2002**, *25*, 695.

(10) Curry, S.; Brick, P.; Franks, N. P. *Biochim. Biophys. Acta* **1999**, *1441*, 131.

(11) Baker, G. A.; Pandey, S.; Kane, M. A.; Maloney, T. D.; Hartnett, A. M.; Bright, F. V. *Biopolymers* **2001**, *59*, 502.

(12) Castner, E. W., Jr.; Maroncelli, M.; Fleming, G. R. *J. Chem. Phys.* **1987**, *86*, 1090.

(13) Prendergast, F. G.; Meyer, M.; Carlson, G. L.; Iida, S.; Potter, J. D. *J. Biol. Chem.* **1983**, *258*, 7541.

(14) Garrison, M. D.; Iuliano, D. J.; Saavedra, S. S.; Truskei, G. A.; Reichert, W. M. *J. Colloid Interface Sci.* **1992**, *148*, 415.

(15) Wang, R.; Sun, S.; Bekos, E. J.; Bright, F. V. *Anal. Chem.* **1995**, *67*, 149.

(16) Jordan, J. D.; Dunbar, R. A.; Bright, F. V. *Anal. Chem.* **1995**, *67*, 2436.

(17) Lundgren, J. S.; Heitz, M. P.; Bright, F. V. *Anal. Chem.* **1995**, *67*, 3775.

(18) Lundgren, J. S.; Bright, F. V. *J. Phys. Chem.* **1996**, *100*, 8580.

(19) Ingersoll, C. M.; Jordan, J. D.; Bright, F. V. *Anal. Chem.* **1996**, *68*, 3194.

(20) Narazaki, R.; Maruyama, T.; Otagiri, M. *Biochim. Biophys. Acta* **1997**, *1338*, 275.

(21) Flora, K.; Brennan, J. D.; Baker, G. A.; Doody, M. A.; Bright, F. V. *Biophys. J.* **1998**, *75*, 1084.

(22) Buzády, A.; Erostyák, J.; Somogyi, B. *Biophys. Chem.* **2001**, *94*, 75.

(23) Pierce, D. W.; Boxer, S. G. *J. Phys. Chem. A* **1992**, *96*, 5560.

(24) Vincent, M.; Gallay, J.; Demchenko, A. P. *J. Fluoresc.* **1997**, *7*, 107S.

(25) Lakowicz, J. R.; Cherek, H. *J. Biol. Chem.* **1980**, *255*, 831.

(26) Vincent, M.; Gilles, A. M.; Li de la Sierra, I. M.; Briozzo, P.; Barzu, O.; Gallay, J. *J. Phys. Chem. B* **2000**, *104*, 11286.

(27) Buzády, A.; Erostyák, J.; Somogyi, B. *Biophys. Chem.* **2000**, *88*, 153.

(28) Kovalenko, S. A.; Eilers-König, N.; Senyushkina, T. A.; Ernsting, N. P. *J. Phys. Chem. A* **2001**, *105*, 4834.

(29) Maroncelli, M. *J. Chem. Phys.* **1991**, *94*, 2084.

(30) Fleming, G. R.; Cho, M. *Annu. Rev. Phys. Chem.* **1996,** *47*, 109.

(31) Viard, M.; Gallay, J.; Vincent, M.; Meyer, O.; Robert, B.; Paternostre, M. *Biophys. J.* **1997**, *73*, 2221.

(32) Willard, D. M.; Riter, R. E.; Levinger, N. E. *J. Am. Chem. Soc.* **1998**, *120*, 4151.

(33) Datta, A.; Pal, S. K.; Mandal, D.; Bhattacharyya, K. *J. Phys. Chem. B* **1998**, *102*, 6114.